Superresolution Multidimensional Imaging with Structured Illumination Microscopy

Aurélie Jost[1,2] and Rainer Heintzmann[1,2,3]

[1]Institute of Physical Chemistry, Abbe Center of Photonics, Friedrich Schiller University, Jena, Germany; email: aurelie.jost@ipht-jena.de, heintzmann@gmail.com

[2]Institute of Photonic Technology, Jena, Germany

[3]Randall Division of Cell and Molecular Biophysics, Kings College London, London, United Kingdom

Annu. Rev. Mater. Res. 2013. 43:261–82

First published online as a Review in Advance on April 29, 2013

The *Annual Review of Materials Research* is online at matsci.annualreviews.org

This article's doi: 10.1146/annurev-matsci-071312-121648

Keywords

Abbe limit, point spread function, PSF, optical transfer function, OTF, optical sectioning, moiré effect

Abstract

The resolution of an optical microscope is fundamentally limited by diffraction. In a conventional wide-field fluorescence microscope, the resolution limit is at best 200 nm. However, modern superresolution methods can bypass this limit. Pointillistic imaging techniques like PALM (photoactivated localization microscopy) and STORM (stochastic optical reconstruction microscopy) do so by precisely localizing each individual molecule in a sample. In contrast, STED uses the stimulated emission process driven to saturation to dramatically reduce the size of the region in the sample that is capable of spontaneously emitting fluorescence. Structured illumination microscopy (SIM) illuminates the sample with a pattern, typically the image of a grating. This computationally removes the out-of-focus blur, a method known as optical sectioning SIM. Furthermore, frequency mixing of the illumination pattern with the sample caused by the moiré effect results in a downmodulation of fine sample detail into the frequency-support region of the detection optical transfer function. High-resolution SIM achieves typically a twofold lateral resolution enhancement. This is further improved by exploiting a nonlinear sample response to the illumination light in SIM. Recent developments of the method allow fast, multicolor, and three-dimensional high-resolution live-cell imaging.

1. INTRODUCTION

Abbe limit: minimum resolvable pitch of a periodic pattern

Wide field (WF): whole field of view under study, as opposed to point scanning

Numerical aperture (NA): an important experimental parameter that is linked to the opening angle

FT: Fourier transformation

Optical sectioning: removal of the out-of-focus blur

STED: stimulated emission depletion

Photoactivated localization microscopy (PALM): a pointillistic localization-based superresolution technique using photoactivatable fluorophores

Stochastic optical reconstruction microscopy (STORM): a pointillistic superresolution technique based on photoswitchable fluorophores

SIM: structured illumination microscopy

Fluorescence microscopy is a very successful method for imaging biological samples. It is very popular because specific targets inside a cell under study can be labeled and are then visible in front of a dark background. It offers good contrast and sensitivity down to the single-molecule regime because the wavelength of the emitted light is slightly different from the excitation wavelength. One section of this review is devoted to detailed explanations on fluorescence. Several fluorescent microscopy techniques exist, and each is tailored for specific applications.

Resolution is one of several parameters that define the performance of an optical microscope. One accepted way to quantify resolution is through the criterion of the Abbe limit. Let's assume that an object is made of thin parallel lines placed at a repetition distance d. When d gets smaller, it is commonly said that the grating gets finer or its spatial frequency increases. The resolution limit is the cutoff distance under which the contrast of the image of this grating will be zero, and the grating will not be visible anymore:

$$d_{\min} = \frac{\lambda}{2\mathrm{NA}}. \qquad 1.$$

$d_{\min}$ is the minimum resolvable distance using a wide-field (WF) fluorescence microscope, when one is using emission light with a wavelength in vacuum of λ and a microscope objective of numerical aperture

$$\mathrm{NA} = n \sin\alpha, \qquad 2.$$

where α is the half opening angle and n is the refractive index of the immersion medium. In a good-quality WF optical microscope ($\lambda = 520$ nm, NA $= 1.4$), $d_{\min}$ is approximately 200 nm. Note that any information, including nonperiodic, can be decomposed as a sum of several periodic components, a mathematical operation termed the Fourier transformation (FT). Even though Abbe's equation (Equation 1) was first conceived for the case of transmission imaging under oblique illumination, the same equation applies just as well to the case of imaging the incoherent fluorescence emission.

The first significant improvement over the classical WF instrument is the confocal microscope (1). It rejects out-of-focus light, thus achieving a better discrimination of the structure along the optical axis, known as optical sectioning. Even though a confocal microscope has in principle the ability to achieve double lateral resolution, it does so extremely inefficiently, thus rendering this theoretical ability practically useless. Another technique, optical coherence tomography (OCT), uses interferometric detection to achieve depth discrimination and is a method well suited for imaging of nonfluorescent layered structures (2). It has the advantage of a large penetration depth, which is a desirable criterion for many applications. OCT has applications in biomedicine (3–5) and material research (6–9). However, in contrast to these techniques, others concentrate on the enhancement of lateral resolution.

A number of superresolution methods have been recently developed (10, 11). They bypass the diffraction limit, resolving structural details spaced at distances well below 100 nm. Stimulated emission depletion (STED) (12), photoactivated localization microscopy (PALM) (13), stochastic optical reconstruction microscopy (STORM) (14), and structured illumination microscopy (SIM) are examples (15, 16) (see **Figure 1**).

In STED, a focused laser beam excites the electrons to an upper level. A doughnut-shaped second beam of a different color de-excites the fluorophores by the stimulated emission process, thus minimizing the region of spontaneous fluorescence, leading to improved resolution (see **Figure 2** and the sidebar, What Is Stimulated Emission?). Pointillistic imaging techniques like PALM and STORM utilize the property that fluorophores can be sparsely randomly activated,

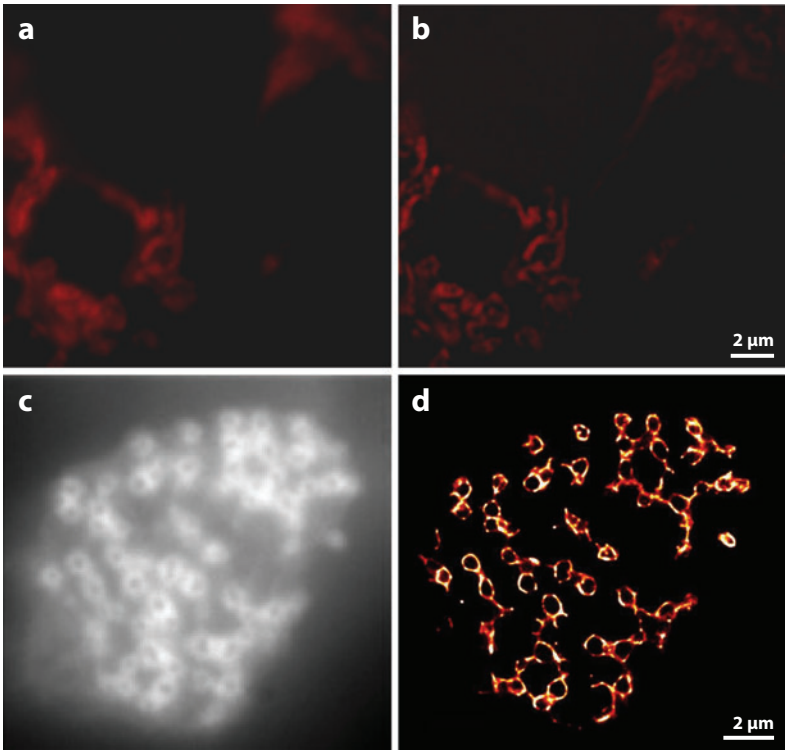

Figure 1

Examples of superresolution images. (*a*,*b*) Images of COS-7 cells labelled with MitoTracker® (samples generously provided by B. Qualmann & M.M. Kessels, Jena University Hospital/Friedrich-Schiller-University, Jena, Germany). (*a*) Wide-field fluorescence image. (*b*) High-resolution SIM reconstruction. Scale bar: 2 µm. (*c*,*d*) Reconstructed images of living THP-1 cells marked with an mCherry construct of a truncated version of Talin. (*c*) Wide-field reconstruction. (*d*) Reconstruction using Bayesian analysis of blinking and bleaching (17). Scale bar: 2 µm. The images in panels *c* and *d* were provided by Dr. Susan Cox.

thus leading to a separation in time of the individual images of the fluorophores. Their positions can be determined very precisely by a fit (e.g., using a Gaussian) with a precision far below the Abbe limit. The result is a pointillistic map of estimated locations, hence the name pointillistic imaging (18). In PALM, this separate activation is achieved through the use of photoactivatable fluorophores, and in STORM with photoswitchable fluorophores (see **Figure 3**).

SIM is another superresolution technique. A commercial structured illumination microscope SIM offers a resolution of the order of 100 nm.

A SIM system can be implemented by simply placing a fine grating in one of the image planes of a standard full-field epifluorescence microscope. Thus, sinusoidal modulation of the light is produced in the sample space. If this illumination is produced by using a coherent laser beam, almost perfect modulation in the sample can be achieved up to the highest spatial frequency.

STED is a point-scanning technique. Its speed is thus limited by its scanning mechanism and the size of the area to be scanned. PALM and STORM are full-field methods requiring hundreds (17) to tens of thousands (13) of individual images. SIM is also a full-field method, but it requires the acquisition of only a few frames, as explained below. It therefore distinguishes itself from the other superresolution techniques by its potentially faster imaging rate.

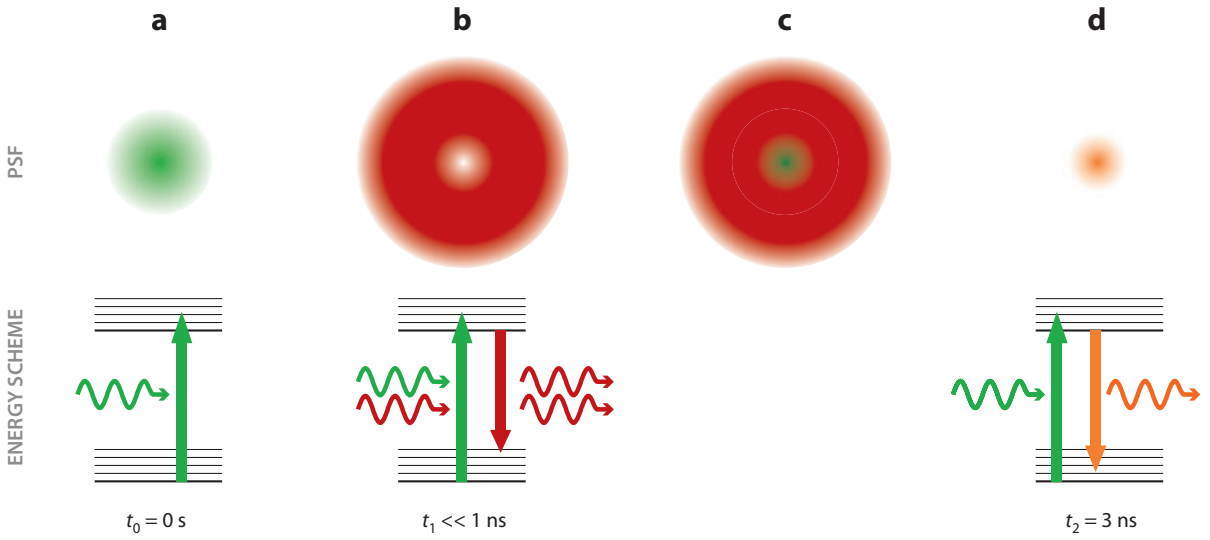

Figure 2

The excitation and de-excitation processes in stimulated emission depletion (STED). (*a*) (*Top*) Excitation point spread function (PSF). Its size is limited by diffraction of the excitation light through the objective. (*Bottom*) Corresponding transition in the Jablonski energy scheme. (*b*) (*Top*) Stimulated emission doughnut-shaped beam. (*Bottom*) The fluorophores within the region of the doughnut are forced to the ground state by the stimulated emission process driven into saturation. Note that the fluorophores in the very center of the doughnut beam do not see any STED light and thus remain in the excited state. (*c*) The two previous beams are superimposed and scanned along the region of interest. (*d*) (*Top*) Effective PSF of the combined effects. (*Bottom*) The fluorophores that have not been de-excited by the STED beam can emit fluorescent photons, which come from a region of much smaller radius. A careful selection of the emission filter can prevent the usually further redshifted stimulated emission light from reaching the detector.

In the remainder of this review, we focus on structured illumination, discussing both theoretical and practical aspects. To make the theoretical description easily understandable, we first introduce some general concepts, namely fluorescence emission, point spread function, resolution, convolution, and optical transfer function. Then we present in detail the SIM methods, optical sectioning, and high resolution. The necessary reconstruction procedure and latest implementations using or inspired by SIM are also discussed.

WHAT IS STIMULATED EMISSION?

Stimulated emission is an alternative radiative process to de-excite electrons, which normally decay through spontaneous emission. For instance, if there is a second incident beam whose photons have an energy $h\nu$ that matches that of the energy gap of the material, then the excited electrons are forced to decay by emitting photons at the same wavelength, phase, and polarization as the incoming photons. Thus, the so-called stimulated emission beam is amplified. This is the core process used for creating a laser (light amplification by stimulated emission of radiation). In STED, if the beams are timed precisely, then some fluorophores can be forced to decay before they can spontaneously emit fluorescent photons. As the photon emitted by stimulated emission will have exactly the frequency (and thus wavelength) of the stimulating photon, it is possible to choose a dedicated STED wavelength range separate from the range reserved for detecting spontaneous emission.

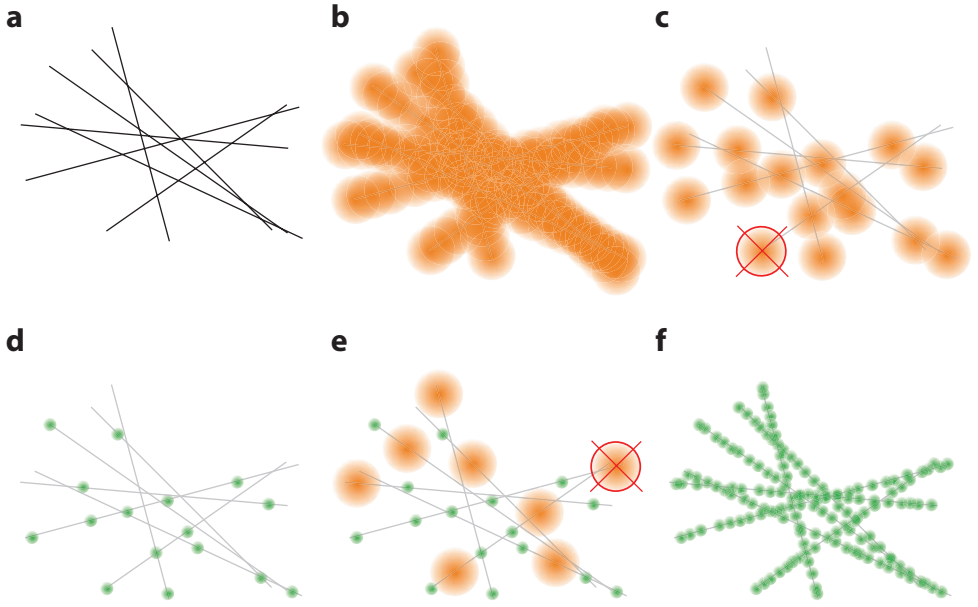

Figure 3

Principles of PALM and STORM. (*a*) Sample consisting of many point sources. (*b*) Simultaneous emission of all the fluorescent markers. (*c*) When photoactivatable (PALM) or photoswitchable (STORM) dyes are used, only very few photons will emit light in a given frame. The images of the individual points will therefore be sparse. A Gaussian fit (*red circle*) is applied to each of these single-molecule images. The center (*red cross*) corresponds to the most probable position of the initial point source. (*d*) Location map after processing of the single frame shown in panel *c*. The small green dots represent the estimation of the position with nanometer precision. (*e*) Another camera frame in which another set of fluorophores are shown. The processing procedure is repeated frame by frame. (*f*) After acquisition and processing of many frames, structural information about the sample is pointillistically reconstructed at a much better resolution.

2. CONCEPTS IN FLUORESCENCE MICROSCOPY

2.1. Fluorescence

Fluorescence has played a crucial role in the success and expansion of microscopy techniques in the past decades. It has become even more important since the discovery that fluorescent proteins such as the green fluorescent protein (GFP) can be used to specifically visualize a protein in a living cell or organism (19).

A fluorescently labeled sample can emit light at a characteristic range of emission wavelengths if it was excited at a different range of excitation wavelengths. The fluorophores, i.e., the fluorescent molecules (also termed dyes) inside the sample, can be targeted to specific parts of the cells. For example, 4′,6-diamidino-2-phenylindole (DAPI) is commonly used to stain the DNA in the nucleus of cells.

Thus, if a filter, matching in its transmission with the range of emission wavelengths, is placed on the detection arm of the microscope, the emitted fluorescence light can pass, whereas scattered light is blocked and only the stained parts of the sample are bright in the resulting image. This has enabled study of the living world with an unprecedented specificity and contrast.

To understand the physics of the fluorescence process, one should have a look at the Jablonski sketch (**Figure 4**), which represents the electronic and vibrational energy levels of a molecule and

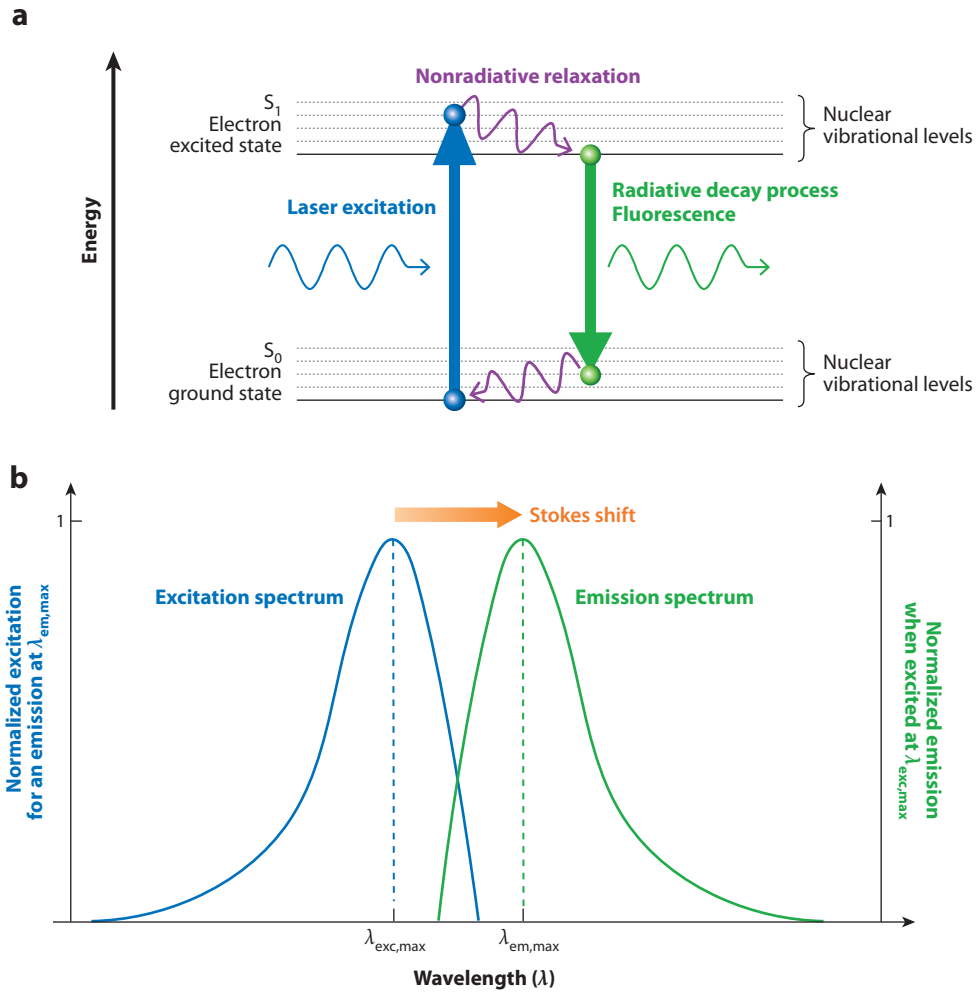

Figure 4

The fluorescence process. (*a*) A simplified Jablonski diagram. An incoming, e.g., blue, photon with energy higher than the gap is absorbed. An electron in the ground state is thus excited. After some very fast (in the range of picoseconds) vibrational relaxation, this molecule reaches the bottom of the excited-level band. Then it can spontaneously decay back to the ground level by emitting a photon. (*b*) Corresponding normalized excitation and emission spectra. The former indicates how well photons inside this wavelength range can excite the fluorophore. In fluorescence, the emitted photons are, to a good approximation, distributed over a spectrum that is obtained via the so-called mirror rule. Due to the internal nonradiative relaxation processes losing energy, it is most probable that the emission wavelength is longer than the excitation wavelength. The difference between their spectral maximas is termed the Stokes shift.

the transitions of the molecules from one state to another. These transitions can be radiative or nonradiative. In **Figure 4**, the sketch has been simplified to depict the fluorescence process only.

To excite the fluorophore, the excitation wavelength has to match the energy difference between the ground and the excited electronic levels—that is, a photon is absorbed. There is an internal relaxation to the lowest-energy (nuclear) vibrational level of the excited state, a process that

typically lasts a few picoseconds. Then the excited electron will decay back to the ground state and, with a certain fluorophore-specific probability (termed quantum efficiency), will emit a photon.

During the two vibrational nonradiative relaxations, some of the initial energy is lost. Therefore, the emission wavelength is longer than in the absorption process. This shift in wavelength is termed the Stokes shift. Fluorescence is so widely used in microscopy because the Stokes shift allows us to select the emitted photons and block the excitation light that otherwise reaches the detection arm either directly or by reflection or scattering.

Point spread function (PSF): image of a single emitter through the system

There is a loss of phase between excitation and emission. Therefore fluorescent light is, unlike back-scattered light, incoherent between different molecules, establishing a very useful linear imaging relationship between the emitted light intensity and the detected image.

There are several methods for fluorescent labeling of biological samples. The binding properties of the dye molecules can be used to specifically stain structures, but they are often attached to antibodies or other ligands. Recently, the genetic modification of proteins to exhibit fluorescence has led to a renaissance of fluorescence in life-cell biology.

It is also possible to fluorescently label a material (20) or to use its autofluorescent properties. There are two categories of fluorescence. The first one is termed primary fluorescence. Here, the material is inherently fluorescent due to inherently present dyes, color centers, lattice dislocations, dopants, or quantum dot structures. In the case of secondary fluorescence, the specimen is treated with a dilute solution of fluorochromes. Secondary fluorescence is sometimes used for polymer and ceramic composites, but in general primary fluorescence is more widespread in material sciences (20). The spectrum of autofluorescence is often broader than that of an artificially introduced single fluorescent dye, which makes it difficult to separate. Autofluorescence is often not desirable in specific labeling experiments of biological samples, as it generates an unspecific background. In some cases, however, autofluorescence can also yield valuable information about the sample. Examples are the imaging of autofluorescence in the retina and of tumors. Many materials, like plastics for instance, exhibit autofluorescence (21–23) upon excitation in the UV and blue bands of the spectrum (20). Lanthanoids or lanthanides (e.g., Er, Eu, La) are also used as natural fluorescence markers. Superresolution microscopy techniques have been applied to image nitrogen vacancy centers in diamond (24).

2.2. Introducing the Point Spread Function and Lateral Resolution

The light emitted by a freely rotating small fluorophore can be seen as being isotropic, i.e., equally distributed over a sphere around each point light source. However, only a fraction of this light can be collected by the optics used for the imaging, whereas the rest is lost. The need is therefore to improve the efficiency of this collection process. An objective with a larger NA collects light coming from a wider range of angles.

Abbe's equation (Equation 1) shows that, to improve the resolution of a WF microscope, it is possible to use higher-NA objectives and a shorter imaging wavelength. There is a very similar dependence for the radius of the central spot of the image of a single emitter. For an NA of 1.4 and a central wavelength of 520 nm, the transverse full width at half-maximum is of the order of 200 nm, which is usually quite close to Abbe's diffraction limit. Note also that the depth of field of a high-NA objective will be short, which can be a disadvantage for some applications. The range in depth over which the beam remains focused is much shorter when a higher-NA objective is used. This can be a disadvantage for some applications that require extended focus.

Each fluorophore can be considered as a point in the sample plane. However, due to diffraction, the resulting image of this point will be blurred. This blurred spot, termed the point spread function (PSF), has (approximately) the shape of an Airy pattern. As a consequence, two fluorophores that

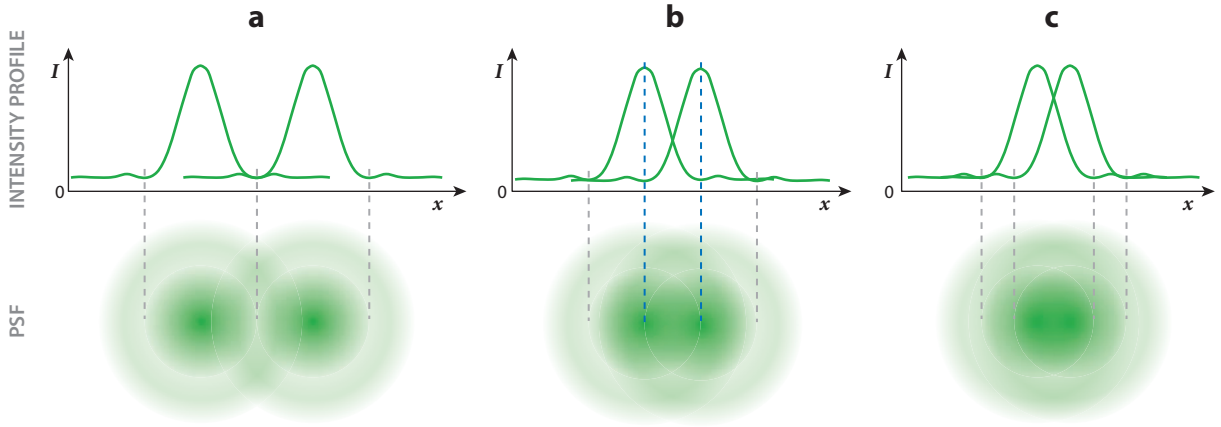

Figure 5

The Rayleigh criterion is another accepted way to define the resolution. (*Bottom*) Airy discs as a model for the point spread functions (PSFs) of two neighboring point sources. (*Top*) The corresponding intensity profile. The gray dashed lines indicate the position of the first minimum. (*a*) The distance between the two points is larger than the resolution limit: They are resolved. (*b*) The two blue dashed lines are separated by a radius of the Airy patterns $R_{\text{Airy}} = \frac{1.22\lambda}{2\text{NA}}$, where λ is the wavelength of light and NA is the numerical aperture. R_{Airy} is the value of the resolution limit when the Rayleigh criterion is used. (*c*) The distance between the two point sources is smaller than the resolution limit.

stand close to each other will produce a wide blurred area, each individual PSF overlapping with its neighbor's. It will be difficult to resolve them, i.e., to discriminate that there are two emitters in this area, and to determine their precise positions (see **Figure 5**).

2.3. Convolution in Optics

One can consider any fluorescent labeled structure as a very high number of points that all emit light in the same way, and each of these points is imaged by a PSF. The PSF can therefore be seen as a "brush" drawing the sample, resulting in a blurry final image. This painting process can be mathematically described as a convolution operation. Convolution in real space has the interesting property of being equivalent to multiplication of the respective Fourier-transformed functions in Fourier space (convolution theorem). The FT of the whole microscope's PSF is termed the optical transfer function (OTF). Indeed, its action is comparable to that of a system's transfer function in electronics. The FT of the sample is multiplied by the OTF of the microscope. The OTF refers to the ability of the imaging system to transfer incoherent intensity information. OTFs have cutoff frequencies. The resolution of an optical system is fundamentally limited by the support region of the OTF, which defines the maximum spatial frequency range that can be transmitted. Each optical element has its own coherent transfer function (CTF), which illustrates the way each element transmits the spatial frequencies of amplitude light waves contained in the incoming signal.

Optical transfer function (OTF): Fourier transform of the point spread function (its support is a measure of the resolution); also referred to as incoherent transfer function

CTF: coherent transfer function

Let us consider a thin convex lens illuminated by parallel rays. The incident beam is a plane wave, and the converging beam is a spherical wave. The converging beam may be seen as a superposition of an infinite number of plane waves of **k**-vectors of the same absolute length (constant wavelength), each one originating from a separate position in the aperture plane of the lens (Huygens' principle). Due to the limited size of the back-focal aperture, or due to the limited size of the lens, their angles vary continuously inside the range of $[-\alpha; \alpha]$, where α is the opening angle as used in Equation 2.

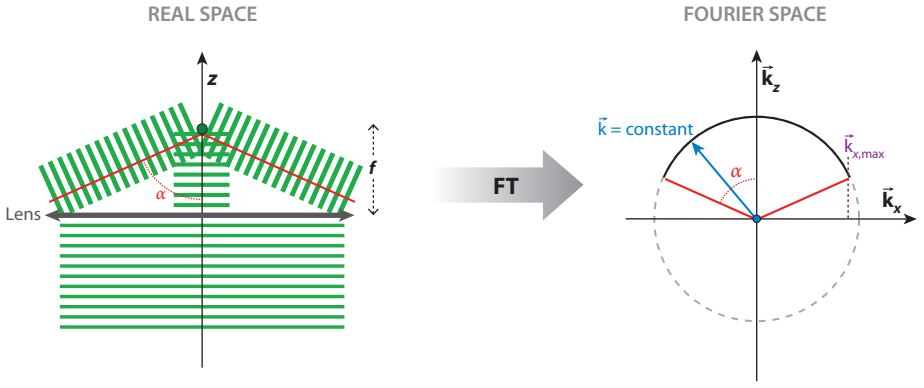

Figure 6

Coherent transfer function (CTF). The converging beam of a lens illuminated by a parallel beam may be seen as an infinite number of plane waves (*green*) of **k**-vectors of the same absolute length (constant wavelength) but whose angles continuously vary inside the range $[-\alpha; \alpha]$, where α is the opening angle. A plane wave is represented by a point in Fourier space. The CTF of the lens represents the way it transmits spatial frequencies contained in the incoming signal. The CTF of a single lens will therefore be a cap of a sphere (same **k**-vector but different angles) (25). Abbreviation: FT, Fourier transformation.

A plane wave is represented by a point in Fourier space. A lens or an objective can collect light coming from all angles within a range defined by its opening angle. In Fourier space, this would be a cap of a sphere (see **Figure 6**). The CTF of a single lens or of an objective will, therefore, be a cap of a sphere, all **k**-vectors with the same length but different angles, and also a cap of a sphere. In **Figure 7**, a cross section through the 3D OTF along the $\mathbf{k}_x$, $\mathbf{k}_z$ plane is shown.

The radius of this sphere is inversely proportional to the wavelength, whereas the opening angle does not depend on the wavelength. Because the excitation light has a shorter wavelength, the size of the **k**-vector in **Figure 6** is accordingly scaled, leading to a scaled version of the excitation OTF. For the moment, we assume a fixed wavelength for the sake of simplicity.

In optics, it is only possible to measure intensities. The relationship between amplitude A and intensity I is

$$\mathrm{I}(x) = \left|\mathrm{A}(x)\right|^2 = \mathrm{A}(x) \cdot \mathrm{A}^*(x), \qquad 3.$$

where * represents the complex conjugate. Therefore, in Fourier domain,

$$\tilde{\mathrm{I}}(k) = \tilde{\mathrm{A}}(k) \otimes \tilde{\mathrm{A}}^*(-k), \qquad 4.$$

where $\sim$ represents the FT operator and $\otimes$ the convolution.

The incoherent OTF is thus obtained by the convolution of the CTF by an inverted and complex conjugated copy of itself (see **Figure 7**). This leads to the missing cone characteristic of a WF fluorescence microscope, which represents spatial frequency around the $\mathbf{k}_z$ axis and is impossible to image. The consequence of this is that planar structures orthogonal to the optical axis yield uniform brightness and, thus, cannot be focused.

One of the goals of microscopy techniques, along with resolution enhancement, i.e., extension of the support region provided by x, y (lateral resolution) and z (axial resolution), is to fill this missing cone. When this goal is achieved, the microscope can perform optical sectioning. Indeed, a fluorescent plane can then be axially resolved. Due to the missing cone, out-of-focus light distributes only to other regions, but its sum does not weaken.

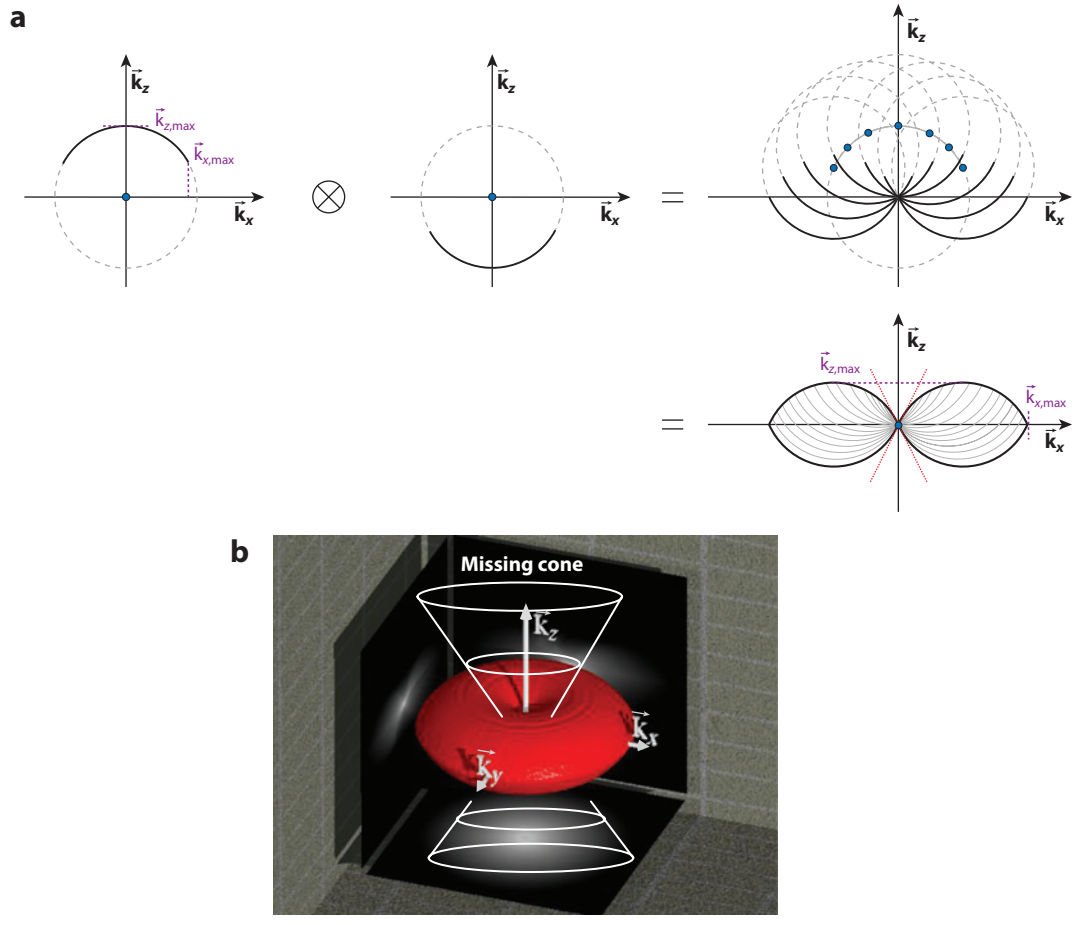

Figure 7

Incoherent optical transfer function (OTF). In optics we measure the intensity, which is the absolute square of the amplitude and can be written as the product of the amplitude with its own complex conjugate. The Fourier transformation of a product is a convolution. Thus, the graphical interpretation of the OTF of a system is obtained by overlaying one function upon the support region of the other (painting one with the other as a "brush"). The missing cone is a characteristic of any classical microscope. It represents spatial frequencies that are not possible to image. One of the goals of recent microscopy techniques, along with resolution enhancement, is to fill out this missing cone (26).

3. THE SIM PRINCIPLE

In structured illumination, the illumination function is not uniform as in standard WF microscopy. The sample is excited with a periodic illumination pattern, often referred to as the grating. The image M can then be expressed as

$$\mathrm{M}(x, y, z) = [\rho(x, y, z) \cdot \mathrm{I}(x, y, z)] \otimes \mathrm{h}(x, y, z), \qquad 5.$$

where ρ is the fluorophore's density, I is the illumination intensity, and h is the PSF.

In the Fourier domain,

$$\tilde{\mathrm{M}}(k_x, k_y, k_z) = [\tilde{\rho}(k_x, k_y, k_z) \otimes \tilde{\mathrm{I}}(k_x, k_y, k_z)] \cdot \tilde{\mathrm{h}}(k_x, k_y, k_z). \qquad 6.$$

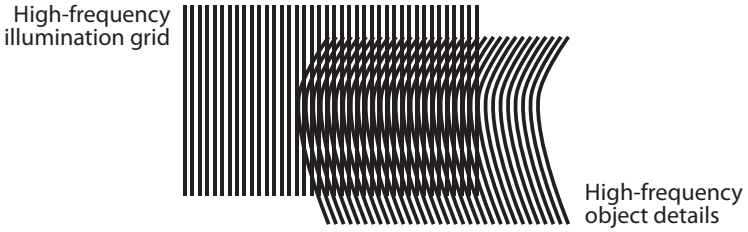

Figure 8

Moiré effect. The superposition of two periodic structures produces a downmodulation of the frequencies; i.e., two structures of high spatial frequency can generate a low spatial frequency in the overlap.

Thanks to the periodic illumination, SIM has an effective OTF with an extended support region from the $\mathbf{k}_x$, $\mathbf{k}_y$ plane and/or the filled-out missing cone. These two achievements are at the core of the two branches of SIM methods, which are presented in detail below.

The first branch of SIM deals with optical sectioning using incoherent light. As a consequence, the contrast of the sinusoidal modulation is high only in the focal plane of the objective. When shifting the grating laterally, the fluorophores that lie in this plane are illuminated by a modulated signal. However, the fluorophores that are away from the focal plane are homogeneously illuminated. Optical sectioning can be achieved with a simple discrimination algorithm (see Section 3.2).

The other branch of SIM deals with high-resolution imaging using the moiré effect to produce lateral, and sometimes axial, resolution enhancement. This effect is based on the frequency mixing of the fine grating with the object (see **Figure 8**). It results in a downmodulation of the high-frequency components in the sample, shifting them into the support region of the OTF of the microscope (27). Thereby, linear SIM can achieve a twofold lateral resolution enhancement compared with conventional WF microscopy (see Section 3.3).

Being a WF method, the main advantage of SIM is that it can be significantly faster than conventional point-scanning microscopic techniques, which are inherently limited in speed by the finite fluorescence lifetime limiting the number of emitted photons that can be generated in the focus. Nevertheless, in SIM one needs to acquire several frames for a single reconstruction; thus, the speed of the method scales with the availability of fast camera technology.

3.1. Setup

The key element of any SIM setup is the patterned excitation. In the classical implementation, the sinusoidal modulation of light is the result of two-beam interference. A phase or amplitude grating can act as an illumination mask. The grating is illuminated by either collimated laser light (for optimum contrast) or incoherent light (for ease of use and sectioning). The grating produces three diffracted beams, which are focused by L_3. They converge in the back focal plane (BFP) of the system of lenses $\{L_3, L_4\}$ (see **Figure 9**). The central spot can be blocked, and the $\pm$ first orders are directed by a dichromatic mirror onto a microscope objective of high NA. The interference of the $\pm$ first orders creates the excitation pattern that illuminates the sample (here corresponding to twice the periodicity of the original grating). The fluorescent light is collected by the same objective. The emission passes through the beamsplitter and a clean-up detection filter, and the fluorescence is imaged through a tube lens onto a camera.

The use of a mechanical grating is, however, not always the preferred solution. It lacks flexibility because changing the period of the grid to adapt to a different wavelength requires changing the components. Moreover, the necessary grating translation and rotation are serious limitations on

Moiré effect: frequency mixing responsible for the resolution enhancement in structured illumination microscopy

BFP: back focal plane

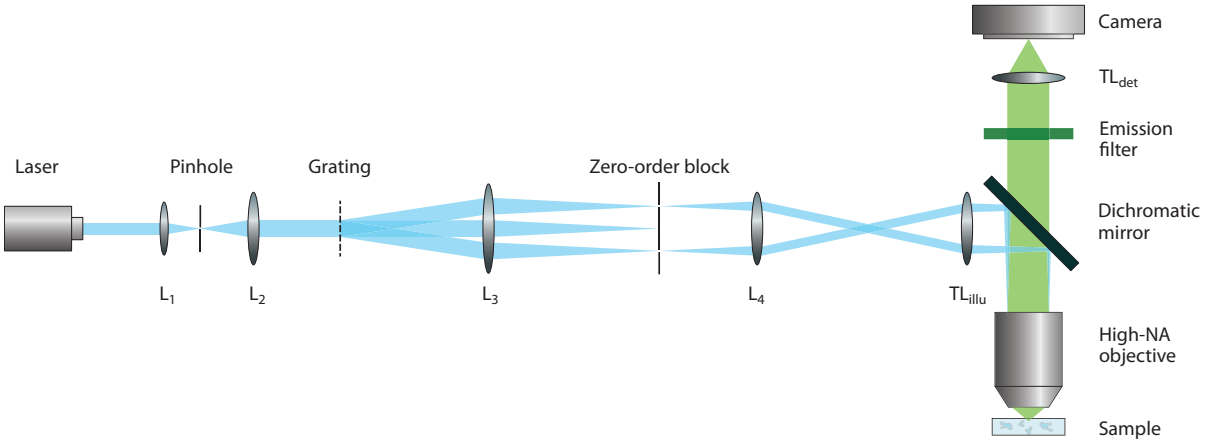

Figure 9

Basic SIM setup. The light source is usually a laser or an incoherent light source. The beam is collimated by L_1 and L_2. A grating produces diffracted beams that are focused in the back focal plane of L_3. There, a mask can be applied that lets only the $\pm$first orders pass. The diffracted beams interfere beyond the objective to produce a periodic high-frequency pattern in the sample. The fluorescence light is filtered and imaged with a camera.

the speed of the system. Using opto-electronical or micromechanical technology instead of a motorized grating is much faster. Therefore, the use of a spatial light modulator (SLM) is an attractive illumination tool for SIM (28). The SLM is a computer-driven opto-electronic device that enables faster changing of the grating position and orientation. SLMs are very useful devices in modern optics and find applications in many different fields (29).

3.2. Optical Sectioning

Here, the illumination light is incoherent, the pattern is relatively coarse, and there is no order-selection aperture, so a pattern is generated with good contrast only in the focal plane (30). The grating is shifted in steps laterally. The step of the shift should be a third of a period, so that after three translations, each region of the focal plane has received the same amount of light in total. During this phase shift, the fluorophores that are in the focal plane experience an intensity modulation, whereas the ones that are out of focus are illuminated with equal brightness through the frames (see **Figure 10**). It is therefore possible to discriminate between them using the following equation (30):

$$I_{sec} = \sqrt{(I_1 - I_2)^2 + (I_2 - I_3)^2 + (I_3 - I_1)^2}, \quad 7.$$

where I_n are the n acquired raw images for one grating position.

The result, I_{sec}, is an optically sectioned image, i.e., an image that only contains in-focus information. The removal of the out-of-focus blur dramatically improves the image's quality. Other discrimination equations have been proposed in Reference 31.

Spatial light modulator (SLM): often used to produce the illumination grating in SIM

Optical sectioning SIM is a powerful method, but it requires the acquisition of three raw images and knowing the shift of the grating that produces the illumination modulation. This poses a limitation to the speed of the method and to applications imaging fast-moving targets. To image fast biological processes, the acquisition time for the three frames has to be kept to a minimum.

A new technique termed picoSIM enables single-shot optical sectioning by utilizing polarization-maintaining properties of fluorescent dyes. Here, instead of being an intensity

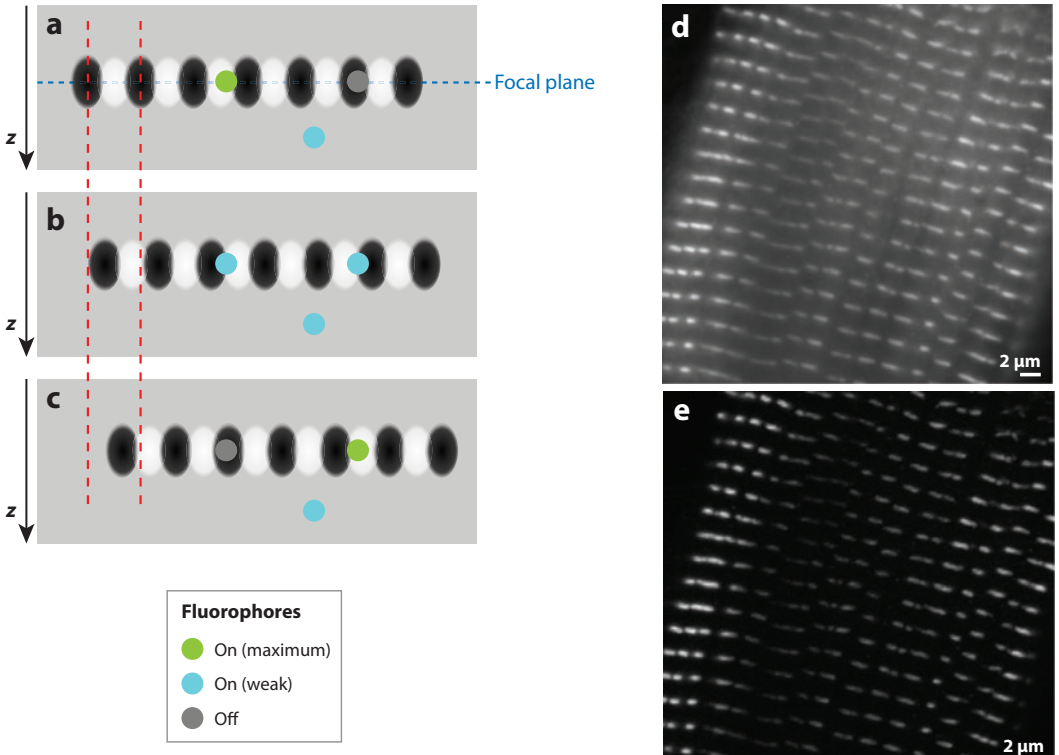

Figure 10

An acquisition series in sectioning SIM shown on an *x*-*z* section through sample space and example of optically sectioned SIM image. (*a*) First time frame: The contrast of the grating is high only in the focal plane. The fluorophores that lie on a bright fringe are efficiently excited and emit light (*green dots*). The fluorophores that lie on a dark area are not excited and do not emit any light (*gray dots*). Outside the focal plane, the contrast of the grating is decreasing, and the illumination is homogeneous. The out-of-focus fluorophores can also be excited and emit light (*cyan dots*). In a standard wide-field system, these out-of-focus fluorophores are responsible for the out-of-focus blur. (*b*) Second time frame: The grating has been shifted by a third of a period. The red dotted lines are markers to help the reader visualize the shift of the grating. The out-of-focus fluorophores are illuminated with the same amount of light as in frame *a*. (*c*) Third time frame: The grating has been shifted by another third of a period. The in-focus fluorophores experience an intensity modulation, whereas the out-of-focus fluorophores are homogeneously illuminated. They can thus be computationally removed. (*d*,*e*) Two images of adult rat cardiomyocytes stained with monoclonal mouse antibodies against the titin epitope T12 and secondary Cy2-conjugated antimouse immunoglobulin antibodies. Data from Reference 30a. (*d*) Wide-field fluorescence image. (*e*) Sectioning SIM reconstruction. One can see the removal of the out-of-focus blur thanks to optical sectioning.

modulation, the grating is replaced by a polarization modulation in which the linear polarization direction changes orientation with lateral position. A polarization-optics-based four-way image splitter then simultaneously leads to four images with different orientations of polarization that are equivalent to four phase positions of an illumination grating (32). The use of an image splitter requires a high-performance camera. In addition, picoSIM requires specific sample preparation with fluorophores that have long rotation correlation time and random orientation.

Another single-shot method exploits the red, green, and blue channels of a CCD camera. Instead of a shifting grating, a color grating is used, hence the name color SIM (CSIM) (33). The latter is, however, hard to implement for fluorescence imaging.

A hybrid technique was proposed to achieve optical sectioning with two images: one standard WF image that carries relatively high frequency information and one structured illumination

image that contains low spatial frequencies that exhibit optical sectioning (34, 35). The two images are then computationally combined, giving it the name HiLo. The advantage of this method is that it requires only two frames, which makes it faster than conventional SIM. A single-shot implementation of this technique has been performed by using two colors for each illumination pattern and two channels for simultaneous acquisition (36). The drawback of this method is remaining cross talk between the −first and +first orders, leading to the potential for creating artifacts.

Incoherent structured illumination has been used to improve the image quality of light-sheet microscopy (37). In this technique, a thin plane of the sample is illuminated from the side using, for instance, a separate cylindrical lens. The benefit of illuminating a single plane is that out-of-focus fluorophores are not excited and photobleaching and phototoxicity are reduced. The combination of light-sheet microscopy with structured illumination further enhances the sectioning capability of light-sheet microscopy while at the same time providing benefits from its low background. Thanks to very fast scanning, this combined method has been successfully applied to studying the morphogenesis of embryos.

The methods described above were tailored toward ease of use and optical sectioning but do not achieve a substantial lateral resolution enhancement. Lateral resolution enhancement is discussed in the next section.

3.3. High Resolution

The moiré effect occurs when the sample is excited with a sinusoidal illumination pattern (see **Figure 8**). In Equation 6, we describe the illumination as follows:

$$\mathrm{I}(\mathbf{r}) = 1 + \cos\left(\mathbf{k}_g \cdot \mathbf{r}\right) = 1 + \frac{1}{2}\left(e^{i\mathbf{k}_g \cdot \mathbf{r}} + e^{-i\mathbf{k}_g \cdot \mathbf{r}}\right), \qquad 8.$$

where $\mathbf{k}_g$ is the grating's **k**-vector.

The multiplication of the illumination pattern and the sample information in real space corresponds to a convolution of their FT in Fourier space. The FT of a sinusoidal grating produced by the interference of two beams consists of three peaks (shown in *blue* in **Figure 11**). Due to the convolution, the same sample information will be "attached" to each of these three peaks. Previously inaccessible sample information outside the detection OTF is thereby shifted into its support region, making it now accessible to optical imaging. A higher-illumination spatial frequency of the excitation grating results in diffraction orders that are spaced further apart. Thus, even higher spatial frequencies of the Fourier-transformed sample information are shifted into the support region of the OTF. If the illumination is achieved through the objective, the maximally possible illumination frequency will be close to the edge of the region of support of the detection OTF (see **Figure 11**). Because of the short wavelength $\mathbf{k}_g$ can in principle be slightly outside, but this is rarely realized in practice. Linear SIM can thus typically achieve a twofold lateral resolution enhancement compared with conventional WF microscopy.

By using nonlinear properties of the dyes, like saturation of fluorescence emission under intense excitation, it is possible to achieve a resolution enhancement limited only by the achieved nonlinearities and the noise. The emission does not depend linearly on the intensity but depends on a nonlinear function of the intensity. Equation 5 must be generalized and becomes

$$\mathrm{M}(x, y, z) = \{\rho(x, y, z) \cdot \mathrm{f}[\mathrm{I}(x, y, z)]\} \otimes \mathrm{h}(x, y, z), \qquad 9.$$

where the action of f distorts the otherwise sinusoidal excitation. This leads to the generation of higher harmonics inside the sample (without any optics being involved here). By the previously described mechanism, sample information gets attached to each of the newly generated delta

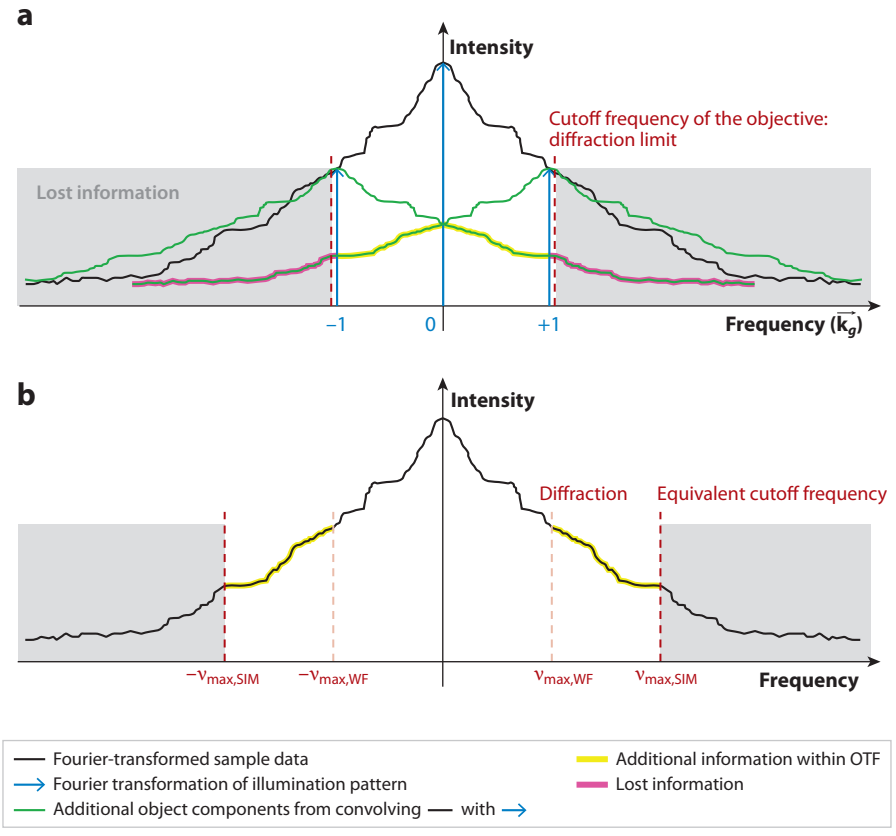

Figure 11

Lateral resolution enhancement. (*a*) Imaging model: The Fourier-transformed sample information (*black*) is convolved with the Fourier transformation of the illumination pattern (*blue*). This results in additional object components (*green*) at the position of the ± first orders. Additional information lies within the support region of the detection optical transfer function (OTF) (*yellow*). Some information is still lost (*magenta*). (*b*) Image reconstruction: The equivalent cutoff frequency is twice as big as that in the wide-field (WF) case. This figure does not show the decay of the OTF with frequency and shows only the cutoff outside its support region.

peaks in Fourier space, which can now be well beyond any limit imposed by optics; i.e., there can theoretically be an infinite number of orders that add information by dragging it into the WF support region. As explained below in more detail, to be able to separate the components and reconstruct the high-resolution image, there should be as many raw images per direction as there are orders in the OTF (38–40). This latter requirement can be weakened (41, 42).

Figure 12*a* shows how two-beam linear SIM modifies the 3D OTF. If the lateral resolution is improved exactly by a factor of two in a two-beam illumination setup, then the missing cone is not filled out. The doubling of the lateral resolution is achieved when the period of the grating is chosen so that the ± first orders lie effectively at the border of the BFP of the objective. In other terms, they can just barely enter the objective.

It is nevertheless possible to achieve optical sectioning with two beams by using a slightly coarser grating so that the orders are not exactly at the limit of the OTF. This configuration does not use the full potential resolution but partially fills out the missing cone as a compromise.

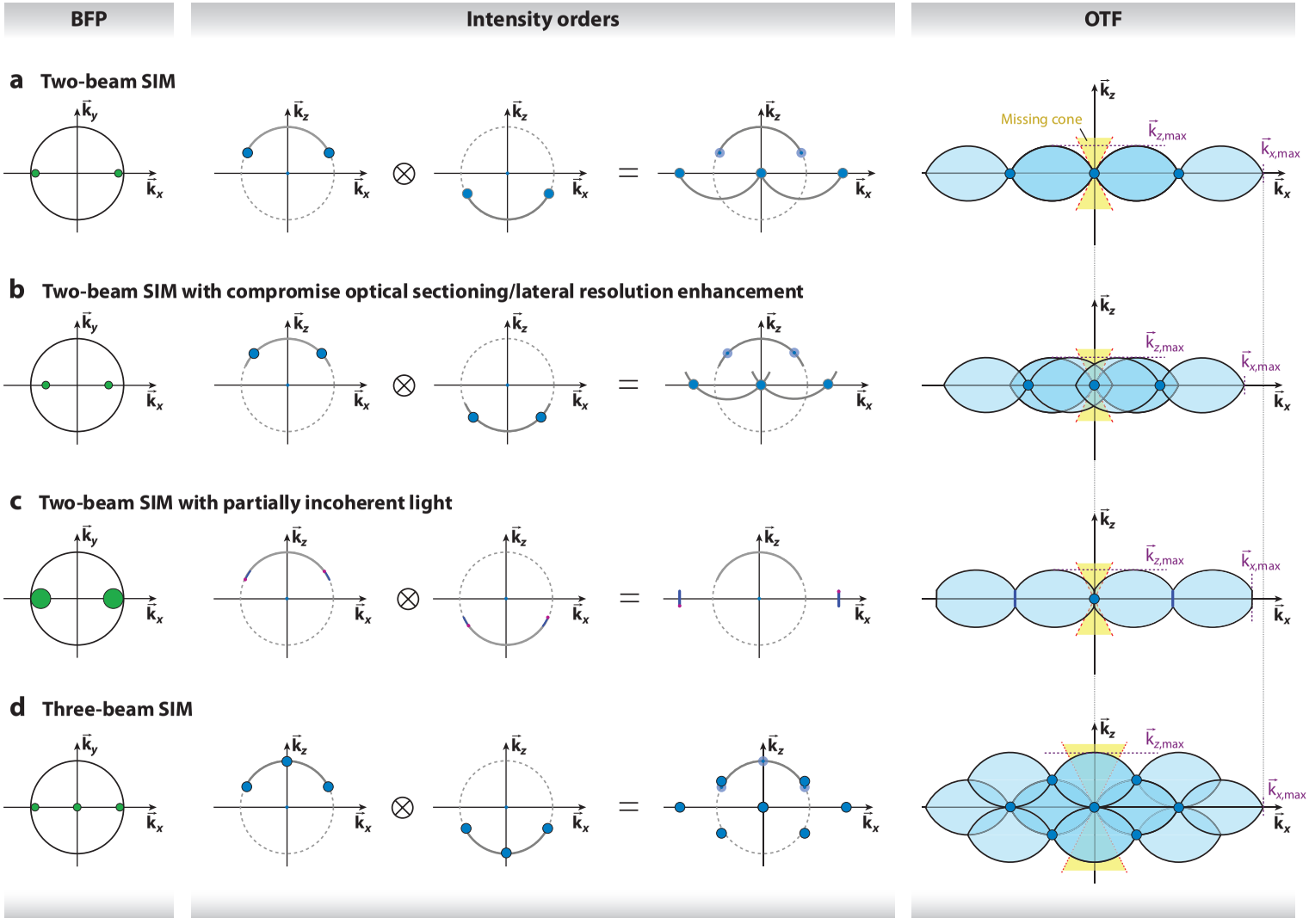

Another method consists of using slightly incoherent light, which produces a smearing of the orders (see **Figure 12*c***). Two common methods to make a laser beam partially incoherent are by coupling it into a shaking multimode optical fiber (43) or by sending it through a rotating diffuser. At the output of such devices, the beam focuses into a homogeneous disk of given diameter and has a certain divergence. The consequence of both methods is that the diffracted orders will not be points in the BFP anymore, but areas. This is directly linked to the spatial incoherence. However, it also means a compromise in resolution because the centers of the diffractions orders will be further away from the border of the BFP.

It is also possible to use three diffracted orders for interference. The resulting illumination pattern will be modulated along the optical axis as well. This is known as the Talbot effect. As can be seen in **Figure 12*d***, the three orders produce a Fourier-transformed illumination function with seven spots. The resulting OTF exhibits both twofold resolution enhancement and filling out of the missing cone. There is even a resolution enhancement along the optical axis: The maximum $\mathbf{k}_z$ frequency in the support region is twice that in the WF case. Three-beam SIM is more commonly used than two beams, as it also allows 3D SIM to be performed.

Using a total internal reflection fluorescence (TIRF) objective enables having high resolution with two-beam illumination and, at the same time, gaining inherent two-dimensionality by the shallow depths of the evanescent excitation field (44). Due to the shallow excitation field, the problem of the missing cone does not apply here. This evanescent illumination is periodically modulated by interference of the two beams, which undergo total internal reflection at the coverslip-embedding medium interface (45). The interference pattern in TIRF can be outside the otherwise inaccessible range of excitation frequencies (46). However, this method limits the imaging to the layer of the sample that is attached to the cover slip.

In conclusion, using a high-resolution sinusoidal grating produces a shift of higher-order components into the support region of the detection OTF of the objective. Thus, one raw image contains the mingled information of n components: $n = 3$ in the two-beam illumination case and $n = 5$ in the three-beam case. In the three-beam case, each pair of orders at $\pm \mathbf{k}_{x,\max}/2$ effectively behaves as one order with a modified detection OTF as they modulate together during phase shift of the illumination structure (47). To separate them, it is best to acquire n images with varying illumination position to reconstruct one final high-resolution image. Three orientations of the grating are required to achieve nearly isotropic lateral resolution enhancement. Hence, one superresolution image requires typically nine raw images in the case of two-beam interference and fifteen raw images in the case of three-beam SIM. The high-resolution image is produced by using a reconstruction algorithm, as explained in the next section.

Figure 12

Optical transfer functions (OTFs) in SIM. (*Left column*) Diffracted orders in the objective's coherent transfer function. (*Middle column*) Corresponding Fourier transformation (FT) of the illumination. Amplitude, not intensity, is depicted here, which means that there is a convolution of the illumination coherent amplitude function with its flipped copy. (*Right column*) Corresponding final OTFs. The FT of the illumination is convolved with the incoherent transfer function (**Figure 6**) of the optical system. (*a*) The zeroth order of the diffraction pattern is blocked by an aperture stop. The orders lie at the border of the back focal plane (BFP). The wide-field (WF) OTF is convolved with three peaks, yielding a twofold lateral resolution enhancement but leaving the missing cone empty. (*b*) With a coarser grating, the orders are placed closer in the BFP. The full-resolution enhancement potential of SIM is not used, but the missing cone is partly filled out. (*c*) When partially incoherent light is used, the orders in the BFP are not points anymore but form disks. This results in a smearing of the orders. The magenta points represent the pair of coherent components. After convolution, the missing cone is also partially filled out. (*d*) If the zeroth order is not blocked, the FT of the illumination yields seven peaks (effectively five for the reconstruction). The latter enables simultaneously optical sectioning and a twofold lateral and axial resolution enhancement. NA denotes numerical aperture, $\mathrm{TL_{det}}$ denotes detection tube lens, and $\mathrm{TL_{illu}}$ denotes illumination tube lens.

All these acquisitions require precise grating movements (translation for the phase shift and rotation for different axial directions) and synchronization with the camera. The speed of the setup can be improved by using a state-of-the art camera and SLM. The readout time of the camera is a major limitation for the acquisition speed. It is advisable to reduce the region of interest to improve the acquisition speed of a system. A method termed I^5S performs high-resolution 3D SIM with an illumination coming from both sides of the sample (48). Kim et al. (49) demonstrated (on simulated data) the possibility of combining SIM with line-scanning microscopy to merge the benefits of both methods. A line-scanning microscope produces optical sectioning in a way similar to the confocal; the difference is that a slit instead of a pinhole is used for rejecting the out-of-focus light. Their simulations show that by scanning a line focus over a grating that is imaged onto the sample, optical sectioning as well as lateral resolution enhancement can be achieved. This principle has been implemented in practice (50).

Achieving higher resolution without using nonlinear properties or making assumptions about the sample is not possible if the excitation pattern is transmitted by the objective. The diffraction orders must lie inside the support region of the excitation OTF. Surface plasmon interference used for generation of the excitation patterns circumvents this limitation. This method is termed plasmonic SIM (51).

3.4. Reconstruction of High-Resolution SIM

As detailed above, each acquired frame contains information on several orders. An image per order and per direction is typically acquired to reconstruct a good-quality high-resolution image. The standard reconstruction algorithm basically separates the orders from the raw data and combines them in the final image.

After background and drift correction, each acquired slice along the optical axis is Fourier transformed. The grating constant and direction are estimated from these data by using a cross-correlation-based technique on preseparated orders. The components are separated and shifted to their correct place in the object spectrum. The algorithm also estimates the strength of each order (height of the *blue arrow* in **Figure 11**) and applies a weighted averaging for overlapping information.

In **Figure 11**, this corresponds to separating each shifted order and the zeroth order, applying a scale factor, shifting them into place, and recombining them with the zeroth order information as sketched in **Figure 11*b***.

The imperfections of the illumination pattern cause problems for the reconstruction algorithms. Distortion of the illumination pattern, caused by aberration, can introduce artifacts in the reconstructed image. The period, direction, and phase shift as well as initial position of the excitation grating can be estimated from the data (52). High contrast of the illumination pattern facilitates the reconstruction. Finally, sample drift and photobleaching are also sources of artifacts.

A method termed blind-SIM was recently developed. It performs image reconstruction without prior knowledge of the illumination pattern (53). This method enables the use of a variety of patterns as random as speckles. Generation of a random speckle field is easily achieved by placing a diffuser in the laser path. This approach is promising because it dramatically simplifies the experimental setup as well as reduces the artifacts in the reconstructed image, although at the expense of requiring many more images and pushing less energy into the high frequencies in each of the images.

4. CONCLUSION AND OUTLOOK

Superresolution microscopy is a quickly evolving field that offers a great variety of techniques for fluorescence imaging of biological samples. Although three methods—STED, pointillism, and SIM—are currently the most popular, there are still many other flavors. This review presents the state of the art in SIM. The benefits of SIM can be separated into two groups: optical sectioning and high resolution. The performance of both variants depends on the reconstruction algorithms. High-resolution SIM reconstruction most specifically requires precise control (or estimation) of many experimental parameters. Sophisticated algorithms that have lately become available are therefore a welcome achievement.

Advances in recent years in SIM have made the technique more and more widespread. Commercial systems are now available, generating new biological insights (54). The most recent achievements have been in live-cell imaging (55). Indeed, to remain a state-of-the-art technique and to meet the needs of biological research, current SIM development aims at speed enhancement, phototoxicity reduction, and practical experimental implementation in addition to further enhancing the resolution (by improving NL SIM) and developing more robust algorithms.

SUMMARY POINTS

1. There are three classes of so-called superresolution microscopy methods that achieve resolution of better than 100 nm: pointillistic techniques (PALM, STORM), STED, and SIM. Each emitter in the sample yields a point spread function (PSF) as its image. The width of the PSF relates to the resolution of the system. The Fourier transformation (FT) of the PSF is the optical transfer function (OTF). The cutoff frequency of the support region of the OTF is a quantitative measure of the OTF and corresponds to the resolution unit, Abbe's resolution in the wide-field case.
2. SIM is a wide-field technique that illuminates the fluorescently labeled biological samples with a patterned intensity, often the image of a grating.
3. The excitation grating is often produced by the interference of two or three plane waves in the plane of focus. These coherent waves originate from diffraction orders in the BFP of the objective.
4. SIM can be divided into two classes: optical sectioning SIM and high-resolution SIM.
5. Optical sectioning SIM typically uses coarse gratings and incoherent light, thus limiting the well-contrasted structure of the pattern to the focal plane.
6. High-resolution SIM achieves enhanced lateral resolution. It requires the acquisition of several raw images that are processed by a sophisticated algorithm to reconstruct a final image.

ACKNOWLEDGMENTS

We thank colleagues S. Shukla, O. Mandula, D. Appelt, R. Förster, and K. Wicker for preparing and proofreading this manuscript and for engaging in critical discussions. Special thanks to our collaborators and colleagues S. Cox, J. Monypenny, B. Qualmann, M.M. Kessels, and H.W. Lu, who prepared the samples and/or acquired and processed the figures. We acknowledge the support of the DFG via project HE3492/3-2.

LITERATURE CITED

1. Minsky M. 1961. Microscopy apparatus. *US Patent No. 3,013,467*
2. Huang D, Swanson EA, Lin CP, Schuman JS, Stinson WG, et al. 1991. Optical coherence tomography. *Science* 254(5035):1178
3. Fercher AF, Hitzenberger CK, Drexler W, Kamp G, Sattmann H. 1993. In vivo optical coherence tomography. *Am. J. Ophthalmol.* 116(1):113–14

4. Discusses optical coherence tomography, the method of choice for imaging of layered structures.

4. Fercher AF. 2010. Optical coherence tomography—development, principles, applications. *Z. Med. Phys.* 20(4):251–76

5. Sergeev AM, Gelikonov VM, Gelikonov GV, Feldchtein FI, Kuranov RV, et al. 1997. In vivo endoscopic OCT imaging of precancer and cancer states of human mucosa. *Opt. Express* 1(13):432–40
6. Bashkansky M, Duncan MD, Kahn M, Lewis D III, Reintjes J. 1997. Subsurface defect detection in ceramics by high-speed high-resolution optical coherent tomography. *Opt. Lett.* 22(1):61–63
7. Dunkers JP, Phelan FR, Sanders DP, Everett MJ, Green WH, et al. 2001. The application of optical coherence tomography to problems in polymer matrix composites. *Opt. Lasers Eng.* 35(3):135–47
8. Stifter D, Burgholzer P, Höglinger O, Götzinger E, Hitzenberger CK. 2003. Polarisation-sensitive optical coherence tomography for material characterisation and strain-field mapping. *Appl. Phys. A: Mater. Sci. Proc.* 76(6):947–51
9. Liang H, Cid M, Cucu R, Dobre G, Podoleanu A, et al. 2005. En-face optical coherence tomography—a novel application of non-invasive imaging to art conservation. *Opt. Express* 13(16):6133–44

10. Presents an overview of several SIM methods.

10. Schermelleh L, Heintzmann R, Leonhardt H. 2010. A guide to super-resolution fluorescence microscopy. *J. Cell Biol.* 190(2):165–75

11. Hirvonen LM, Smith TA. 2011. Imaging on the nanoscale: super-resolution fluorescence microscopy. *Aust. J. Chem.* 64(1):41–45
12. Hell SW, Wichmann J. 1994. Breaking the diffraction resolution limit by stimulated emission: stimulated-emission-depletion fluorescence microscopy. *Opt. Lett.* 19(11):780–82
13. Betzig E, Patterson GH, Sougrat R, Lindwasser OW, Olenych S, et al. 2006. Imaging intracellular fluorescent proteins at nanometer resolution. *Science* 313(5793):1642
14. Rust MJ, Bates M, Zhuang X. 2006. Sub-diffraction-limit imaging by stochastic optical reconstruction microscopy (STORM). *Nat. Methods* 3(10):793–96

15, 16. Inaugurated the field of high-resolution fluorescence structured illumination.

15. Heintzmann R, Cremer CG. 1999. Laterally modulated excitation microscopy: improvement of resolution by using a diffraction grating. *Proc. SPIE* 3568:185

16. Gustafsson MGL. 2000. Surpassing the lateral resolution limit by a factor of two using structured illumination microscopy. *J. Microsc.* 198(2):82–87

17. Cox S, Rosten E, Monypenny J, Jovanovic-Talisman T, Burnette DT, et al. 2011. Bayesian localization microscopy reveals nanoscale podosome dynamics. *Nat. Methods* 9(2):195–200
18. Lidke KA, Rieger B, Jovin TM, Heintzmann R. 2005. Superresolution by localization of quantum dots using blinking statistics. *Opt. Express* 13(18):7052–62
19. Chalfie M, Tu Y, Euskirchen G, Ward WW, Prasher DC. 1994. Green fluorescent protein as a marker for gene expression. *Science* 263(5148):802–5
20. Richardson JH. 1971. *Optical Microscopy for the Materials Sciences*. New York: M. Dekker
21. Piruska A, Nikcevic I, Lee SH, Ahn C, Heineman WR, et al. 2005. The autofluorescence of plastic materials and chips measured under laser irradiation. *Lab Chip* 5(12):1348–54
22. Hawkins KR, Yager P. 2003. Nonlinear decrease of background fluorescence in polymer thin-films—a survey of materials and how they can complicate fluorescence detection in μTAS. *Lab Chip* 3(4):248–52
23. Wabuyele MB, Ford SM, Stryjewski W, Barrow J, Soper SA. 2001. Single molecule detection of double-stranded DNA in poly (methylmethacrylate) and polycarbonate microfluidic devices. *Electrophoresis* 22(18):3939–48

24. Applies a super-resolution STED microscope to imaging of diamonds.

24. Rittweger E, Han KY, Irvine SE, Eggeling C, Hell SW. 2009. STED microscopy reveals crystal colour centres with nanometric resolution. *Nat. Photonics* 3(3):144–47

25. Gross H, Singer W, Totzeck M, Blechinger F, Achtner B. 2005. *Handbook of Optical Systems*. Weinheim, Germany: Wiley-VCH

26. Heintzmann R. 1999. *Resolution Enhancement of Biological Light Microscopic Data*. Germany: Rupertus Carola University of Heidelberg
27. Heintzmann R. 2006. Structured illumination methods. In *Handbook of Biological Confocal Microscopy*, ed. J Pawley, pp. 265–79. New York: Springer
28. Kner P, Chhun BB, Griffis ER, Winoto L, Gustafsson MGL. 2009. Super-resolution video microscopy of live cells by structured illumination. *Nat. Methods* 6(5):339
29. Schausberger SE, Heise B, Maurer C, Bernet S, Ritsch-Marte M, Stifter D. 2010. Flexible contrast for low-coherence interference microscopy by Fourier-plane filtering with a spatial light modulator. *Opt. Lett.* 35(24):4154–56
30. Neil MAA, Juskaitis R, Wilson T. 1997. Method of obtaining optical sectioning by using structured light in a conventional microscope. *Opt. Lett.* 22(24):1905–7
30a. Appelt D, Heintzmann R. 2013. Structured illumination microscopy (SIM). In *Encyclopedia of Biophysics*, ed. G Roberts. Berlin/Heidelberg: Springer
31. Heintzmann R, Benedetti PA. 2006. High-resolution image reconstruction in fluorescence microscopy with patterned excitation. *Appl. Opt.* 45(20):5037–45
32. Wicker K, Heintzmann R. 2010. Single-shot optical sectioning using polarization-coded structured illumination. *J. Opt.* 12:84010
33. Krzewina LG, Kim MK. 2006. Single-exposure optical sectioning by color structured illumination microscopy. *Opt. Lett.* 31(4):477–79
34. Lim D, Chu KK, Mertz J. 2008. Wide-field fluorescence sectioning with hybrid speckle and uniform-illumination microscopy. *Opt. Lett.* 33(16):1819–21
35. Mertz J. 2011. Optical sectioning microscopy with planar or structured illumination. *Nat. Methods* 8(10):811–19
36. Muro E, Vermeulen P, Ioannou A, Skourides P, Dubertret B, et al. 2011. Single-shot optical sectioning using two-color probes in HiLo fluorescence microscopy. *Biophys. J.* 100(11):2810–19
37. Keller PJ, Schmidt AD, Santella A, Khairy K, Bao Z, et al. 2010. Fast, high-contrast imaging of animal development with scanned light sheet-based structured-illumination microscopy. *Nat. Methods* 7(8):637–42
38. Rego E, Shao L, Macklin J, Winoto L, Johansson G, et al. 2011. Nonlinear structured-illumination microscopy with a photoswitchable protein reveals cellular structures at 50-nm resolution. *Proc. Natl. Acad. Sci. USA* 109(3):E135–43
39. Heintzmann R, Jovin TM, Cremer C. 2002. Saturated patterned excitation microscopy—a concept for optical resolution improvement. *J. Opt. Soc. Am. A* 19(8):1599–609
40. Hirvonen L, Mandula O, Wicker K, Heintzmann R. 2008. Structured illumination microscopy using photoswitchable fluorescent proteins. *Proc. SPIE* 6861:68610L
41. Heintzmann R. 2003. Saturated patterned excitation microscopy with two-dimensional excitation patterns. *Micron* 34(6–7):283–91
42. Orieux F, Sepulveda E, Loriette V, Dubertret B, Olivo-Marin J-C. 2012. Bayesian estimation for optimized structured illumination microscopy. *IEEE Trans. Image Proc.: Publ. IEEE Signal Proc. Soc.* 21(2):601–14
43. Shao L, Kner P, Rego EH, Gustafsson MGL. 2011. Super-resolution 3D microscopy of live whole cells using structured illumination. *Nat. Methods* 1734(5):1–5
44. Axelrod D. 1981. Cell-substrate contacts illuminated by total internal reflection fluorescence. *J. Cell Biol.* 89(1):141–45
45. Cragg GE, So PTC. 2000. Lateral resolution enhancement with standing evanescent waves. *Opt. Lett.* 25(1):46–48
46. Fiolka R, Beck M, Stemmer A. 2008. Structured illumination in total internal reflection fluorescence microscopy using a spatial light modulator. *Opt. Lett.* 33(14):1629–31
47. Gustafsson MGL, Shao L, Carlton PM, Wang CJ, Golubovskaya IN, et al. 2008. Three-dimensional resolution doubling in wide-field fluorescence microscopy by structured illumination. *Biophys. J.* 94(12):4957–70
48. Shao L, Isaac B, Uzawa S, Agard DA, Sedat JW, Gustafsson MGL. 2008. I5S: wide-field light microscopy with 100-nm-scale resolution in three dimensions. *Biophys. J.* 94(12):4971–83

30. Introduces the optical sectioning SIM idea.

49. Kim T, Gweon DG, Lee JH. 2009. Enhancement of fluorescence confocal scanning microscopy lateral resolution by use of structured illumination. *Meas. Sci. Technol.* 20:55501
50. Mandula O, Kielhorn M, Wicker K, Krampert G, Kleppe I, Heintzmann R. 2012. Line scan—structured illumination microscopy super-resolution imaging in thick fluorescent samples. *Opt. Express* 20(22):24167–74
51. Wei F, Liu Z. 2010. Plasmonic structured illumination microscopy. *Nano Lett.* 10(7):2531–36
52. Wicker K, Mandula O, Best G, Fiolka R, Heintzmann R. 2013. Phase optimisation for structured illumination microscopy. *Opt. Express* 21(2):2032–49
53. Mudry E, Belkebir K, Girard J, Savatier J, Le Moal E, et al. 2012. Structured illumination microscopy using unknown speckle patterns. *Nat. Photonics* 6(5):312–15
54. Schermelleh L, Carlton PM, Haase S, Shao L, Winoto L, et al. 2008. Subdiffraction multicolor imaging of the nuclear periphery with 3D structured illumination microscopy. *Science* 320(5881):1332
55. Rahman M, Abd-El-Barr M, Mack V, Tkaczyk T, Sokolov K, et al. 2005. Optical imaging of cervical pre-cancers with structured illumination: an integrated approach. *Gynecol. Oncol.* 99(3):S112–15

Annual Review of
Materials Research

Volume 43, 2013

Contents

Current Interest